Int. J. Appl. Math. Comput. Sci., 2024, Vol. 34, No. 1, 29–43
DOI: 10.61822/amcs-2024-0003

amcs

DYNAMIC SLIDING MODE CONTROL BASED ON A FULL–ORDER OBSERVER: UNDERACTUATED ELECTRO–MECHANICAL SYSTEM REGULATION

PATRICIO ORDAZ [a], HUGO ROMERO-TREJO [a], CARLOS CUVAS [a,*], OMAR SANDRE [a]

[a] Institute of Basic Sciences and Engineering
Autonomous University of Hidalgo State
Pachuca de Soto, Hidalgo, 42184, Mexico
e-mail: {jesus_ordaz,rhugo,carlos_cuvas,omar_sandre}@uaeh.edu.mx

This paper concerns the synthesis of a nonlinear robust output controller based on a full-order observer for a class of uncertain disturbed systems. The proposed method guarantees that, in finite time, the system trajectories go inside a minimal neighborhood ultimately bounded. To this end, the attractive ellipsoid method is enhanced by applying the dynamic sliding mode control performance properties. Furthermore, in order to guarantee the stability of the trajectory around the trivial solution in the uniform-ultimately bounded sense, the feasibility of a specific matrix inequality problem is provided. With this feasible set of matrix inequalities, the separation principle of the controller/observer scheme considered also holds. To achieve a system performance improvement, a numerical algorithm based on the small size ultimate bound is presented. Finally, to illustrate the theoretical performance of the designed controller/observer, a numerical example dealing with the stabilization of a disturbed electromechanical system with uncertain and unmodeled dynamics is presented.

Keywords: output feedback and observers, sliding mode control, attractive ellipsoid method, uncertain systems, nonlinear systems.

1. Introduction

In situations where we deal with external disturbances or uncertain models when designing a control system, the stabilization near the trivial solution of the controlled system is not guaranteed (Haddad and Chellaboina, 2011; Poznyak *et al.*, 2014; Utkin *et al.*, 2020). In this case, only a bound of the trajectories in some neighborhood of a stable state can be held for the analysis of the nonlinear systems; this concept is known as the ultimate uniform bounded stability (UUB-stability) (Haddad and Chellaboina, 2011). Furthermore, to improve the system trajectories' behavior in terms of the UUB-stability, many controllers based on different approaches have been presented: such is the case of those using sliding mode control (SMC) theory (Utkin *et al.*, 2020), or controllers developed in the frame of the attractive ellipsoid method (AEM) (Sánchez *et al.*, 2019; Poznyak *et al.*, 2014). In this order of ideas, SMC rejects all the external matched bounded disturbances, nevertheless, it produces the well-known chattering effect increasing considerably actuators' wastage (Utkin *et al.*, 2020).

In the last decades, dynamic sliding mode control (DSMC), high order, and integral SMC have been introduced in order to reduce this adverse effect (Utkin *et al.*, 2020). Cao *et al.* (2023) focus on achieving sampled-data stabilization for a class of nonlinear systems under arbitrary sampling periods. This is accomplished by introducing Euler's approximation for unmeasured states and constructing coordinate transformations for the continuous system.

According to the traditional state observation problem, in sliding mode observers (SMOs) state estimation is required to observe the unmeasured state variables (Choi and Ro, 2005; Jafari and Mobayen, 2019; Liu and Khalil, 2019). A special case of SMO is the connection with robust design, where robust performance is achieved by combining concepts of linear matrix inequalities (LMIs) and sliding manifold design (Silva *et al.*, 2009; Choi and Ro, 2005; Jafari and Mobayen, 2019). On the other hand, the design of robust

*Corresponding author

controllers/observers based on the AEM encompasses the matrix inequalities issues (Poznyak *et al.*, 2014; Ordaz *et al.*, 2019). Nevertheless, controllers based on the AEM may provoke a high gain effect in the control signal, particularly when the control design involves state estimation (Poznyak *et al.*, 2014). However, in order to preserve the lifetime of the actuators, it is not recommendable to use controllers with high gain effects and/or those producing large breadth chattering effects.

Nowadays, the problem of reducing the effects of uncertain dynamics and/or external disturbances is addressed by means of robust control approaches, such as output sliding mode control or controller/observer schemes based on Luenberger's theory and the AEM (Tsinias and Theodosis, 2016; Sánchez *et al.*, 2019; Andrade-Da Silva *et al.*, 2009), or combining SMC, the fuzzy control approach (Zhang *et al.*, 2022), and other sophisticated schemes (Peng *et al.*, 2021; Kukurowski *et al.*, 2022). As mentioned above, one of the most relevant results on linear or nonlinear systems is the controller/observer for output regulation. This approach brings about the separation principle, and it has been studied to be satisfied for nonlinear and uncertain systems (Atassi and Khalil, 1999). Different approaches that seem to have a very similar format to the linear case are the AEM algorithm or methods based on LMIs or bilinear matrix inequalities (BMIs) (Sánchez *et al.*, 2019; Ordaz *et al.*, 2019; Poznyak *et al.*, 2014; Choi and Ro, 2005).

Indeed, if there exists some relation between the storage function and its variations having a decreasing behavior, then some kind of stability is guaranteed (Utkin *et al.*, 2020; Haddad and Chellaboina, 2011).

Thus, if the stability analysis is formulated as the solution of an LMI problem, the feasibility of this one is a necessary fact to be guaranteed.

In this context, the main contributions and features of this paper are listed below:

- A nonlinear robust controller/observer is synthesized, which guarantees the so-called UUB-stability, and the closed-loop system considered has a quasi-minimal[1] ultimate bound.
- The adverse effects related to the chattering phenomenon, external disturbances and/or uncertain dynamics, are significantly reduced by summarizing the high gain properties obtained from the AEM approach and robustness provided by the DSMC.
- The separation principle of the designed robust controller/observer scheme is shown through the BMI feasibility process.

Another feature of the paper is a comparative study. This one is presented in order to validate the performance of the proposed controller/observer scheme (in terms of error analysis and energy consumption).

The outline of this paper is as follows. Section 2 presents the dynamic system description, some useful mathematical background, and the problem statements. The main contribution of this paper is introduced in Section 3. Next, Section 4 is devoted to describe the numerical aspects to obtain the quasi-minimal ellipsoidal matrix. The theoretical results are validated in a numerical benchmark presented in Section 5. Finally, the concluding remarks are given.

2. Preliminaries and problem statement

Consider the nonlinear system with external dynamic uncertainties which is governed by the ordinary differential equation

$$\begin{aligned} \dot{x} &= \mathbf{A}x + \mathbf{B}u + \xi_x, \quad x(0) = x_0, \\ y &= \mathbf{C}x + \xi_y, \end{aligned} \tag{1}$$

where matrices and vectors have the following structure:

$$\mathbf{A} = \begin{bmatrix} \mathbf{A}_{11} & \mathbf{A}_{12} \\ \mathbf{A}_{21} & \mathbf{A}_{22} \end{bmatrix}, \qquad \mathbf{B} = \begin{bmatrix} \mathbf{0}_{(n-m)\times m} \\ \mathbf{B}_2 \end{bmatrix},$$

$$\mathbf{C} = \begin{bmatrix} \mathbf{C}_1 & \mathbf{C}_2 \end{bmatrix}, \qquad \xi_x = \begin{bmatrix} f_1(x) + \zeta_1(x,t) \\ f_2(x) + \zeta_2(x,t) \end{bmatrix},$$

with $x = [x_1^\intercal,\ x_2^\intercal]^\intercal$, $x_1 \in \mathbb{R}^{n-m}$, and $x_2 \in \mathbb{R}^m$ being blocks of the connected manifold $x \in X$ of dimension $n \in \mathbb{N}$. The matrices $\mathbf{A}_{11} \in \mathbb{R}^{(n-m)\times(n-m)}$, $\mathbf{A}_{12} \in \mathbb{R}^{(n-m)\times m}$, $\mathbf{A}_{21} \in \mathbb{R}^{m\times(n-m)}$ and $\mathbf{A}_{22} \in \mathbb{R}^{m\times m}$ are blocks of $\mathbf{A} \in \mathbb{R}^{n\times n}$, which is associated with the system state x.

The control input is given by $u \in \mathbb{R}^m$, $m \in \mathbb{N}$, and its realizing matrix is denoted by $\mathbf{B}$, where block $\mathbf{B}_2 \in \mathbb{R}^{m\times m}$ is invertible. The measured output $y \in \mathbb{R}^p$ is associated with the output matrix $\mathbf{C} \in \mathbb{R}^{p\times n}$, whereas $\xi_y \in \mathbb{R}^p$ defines the external disturbances. The nonlinear and uncertain dynamics are represented by f_i and ζ_i, where the index $i = 1, 2$ associates the blocks x_1 and x_2, respectively. The nonlinear functions f_i fulfill the trivial solution $f_i(0) = 0$. Hereafter it is assumed that

$$\|\xi_x\|^2 \le c_1 + c_2 \|x\|^2, \quad \|\xi_y\|^2 \le c_3, \tag{2}$$

at least from the local point of view. Furthermore, the system (1) is assumed to be controllable and observable. In this way, the designed controller must attenuate both the external disturbances and uncertain dynamics, with the latter including unmatched uncertainties. Thus, the use of the estimate of the unmeasured state variables in the control design improves the closed-loop system performance, and this is the justification of the design of

[1] The quasi-minimal bound is not minimal, but it is around the minimal solution.

a full-order observer. The state estimate is given by an observer of a full order defined by

$$\dot{\hat{x}} = \mathbf{A}\hat{x} + \mathbf{B}u + \mathbf{L}\left(y - \mathbf{C}\hat{x}\right), \qquad \hat{x}(0) = \hat{x}_0, \tag{3}$$

where $\mathbf{L} = \left[\mathbf{L}_1^\intercal,\ \mathbf{L}_2^\intercal\right]^\intercal$ is defined here as the observer gain-matrix, also to be designed, with $\mathbf{L}_1 \in \mathbb{R}^{(n-m)\times p}$ and $\mathbf{L}_2 \in \mathbb{R}^{m\times p}$. In order to match it with the system (1) and considering the error function $e = x - \hat{x}$, the previous observer can be rewritten in the extended form as follows:

$$\begin{aligned}\dot{\hat{x}}_1 &= \mathbf{A}_{11}\hat{x}_1 + \mathbf{A}_{12}\hat{x}_2 \\ &\quad + \mathbf{L}_1\mathbf{C}_1 e_1 + \mathbf{L}_1\mathbf{C}_2 e_2 + \mathbf{L}_1\xi_y, \\ \dot{\hat{x}}_2 &= \mathbf{A}_{21}\hat{x}_1 + \mathbf{A}_{22}\hat{x}_2 \\ &\quad + \mathbf{L}_2\mathbf{C}_1 e_1 + \mathbf{L}_2\mathbf{C}_2 e_2 + \mathbf{L}_2\xi_y + \mathbf{B}_2 u.\end{aligned} \tag{4}$$

Remark 1. In the previous equations the estimation errors $e_1 \in \mathbb{R}^{n-m}$ and $e_2 \in \mathbb{R}^m$ are used, but in both the cases, the unavailable state variables are restricted by the matrices $\mathbf{C}_1$ and $\mathbf{C}_2$, respectively.

To see this, consider the nonsingular transformation $\bar{x} = \mathbf{\Gamma}\hat{x}$, where $\mathbf{\Gamma} \in \mathbb{R}^{n\times n}$ is given as

$$\mathbf{\Gamma} = \begin{pmatrix} \mathbf{N}_\mathbf{C}^\intercal \\ \mathbf{C} \end{pmatrix},$$

with $\mathbf{N}_\mathbf{C} \in \mathbb{R}^{n\times(n-p)}$ as the null-space of the output matrix $\mathbf{C}$. In this way, the estimated system (3) can be expressed in the new basis changed to $\bar{x}^\intercal = \left[\bar{x}_1^\intercal \quad \bar{x}_2^\intercal\right]$, where $\bar{x}_1 \in \mathbb{R}^{n-p}$ should be estimated on-line using the available information $\bar{x}_2 \in \mathbb{R}^p$. Thus, the state estimate can be expressed as

$$\dot{\bar{x}} = \mathcal{A}\bar{x} + \mathcal{B}u + \mathcal{L}\left(y - \mathcal{C}\bar{x}\right), \quad \bar{x}(0) = \mathbf{\Gamma}\bar{x}_0, \tag{5}$$

and the system output by $y = \mathcal{C}\bar{x}$, where $\mathcal{A} = \mathbf{\Gamma}\mathbf{A}\mathbf{\Gamma}^{-1}$, $\mathcal{B} = \mathbf{\Gamma}\mathbf{B}, \mathcal{C} = \mathbf{C}\mathbf{\Gamma}^{-1}$ and $\mathcal{L} = \mathbf{\Gamma}\mathbf{L}$. The matrices involved in (5) have the following structure:

$$\begin{aligned}\mathcal{A} &= \begin{bmatrix}\mathcal{A}_{11} & \mathcal{A}_{12} \\ \mathcal{A}_{21} & \mathcal{A}_{22}\end{bmatrix}, & \mathcal{C} &= \begin{bmatrix}\mathbf{0} & \mathbf{I}_p\end{bmatrix}, \\ \mathcal{B} &= \begin{bmatrix}\mathcal{B}_1 \\ \mathcal{B}_2\end{bmatrix}, & \mathcal{L} &= \begin{bmatrix}\mathcal{L}_1 \\ \mathcal{L}_2\end{bmatrix},\end{aligned} \tag{6}$$

with appropriate matrix dimensions. Thus, (5) can be written as

$$\begin{aligned}\dot{\bar{x}}_1 &= \mathcal{A}_{11}\bar{x}_1 + \mathcal{A}_{12}\bar{x}_2 + \mathcal{L}_2\mathcal{C}_2 e_2 + \mathcal{L}_1\xi_y + \mathcal{B}_1 u, \\ \dot{\bar{x}}_2 &= \mathcal{A}_{21}\bar{x}_1 + \mathcal{A}_{22}\bar{x}_2 + \mathcal{L}_2\mathcal{C}_2 e_2 + \mathcal{L}_2\xi_y + \mathcal{B}_2 u.\end{aligned} \tag{7}$$

Equation (7) indicates that, as previously suggested, the unmeasured state variables do not play any role in the dynamic estimation algorithm.

Definition 1. (*Attractive ellipsoid (Poznyak* et al.*, 2014)*) The ellipsoid $\mathcal{E}\left(0, \bar{\mathbf{P}}^{-1}\right) = \{x \in \mathbb{R}^n : x^\intercal\bar{\mathbf{P}}x \le 1,\ 0 < \bar{\mathbf{P}} = \bar{\mathbf{P}}^\intercal\}$ with the center at the origin and the corresponding $n \times n$ ellipsoidal matrix $\bar{\mathbf{P}}$ is attractive for some dynamic system if, for any trajectory $\{x\}_{t\ge0}$, the property $\limsup_{t\to\infty} x^\intercal(t)\bar{\mathbf{P}}x(t) \le 1$ holds.

Next, UUB-stability is defined.

Definition 2. (*Ultimate uniform bounded stability (Haddad and Chellaboina, 2008)*) The system trajectory $x(t)$ of the system (1) is stable around the origin if

$$\|x(t_0)\| \le a \Longrightarrow \|x(t)\| \le b, \quad \forall t \ge t_0 + T,$$

for positive $b, c \in \mathbb{R}$, $a \in (0, c)$, and $T = T(a, b)$ independent of t_0.

However, one problem of SMC is the chattering phenomenon, an effect that is considerably reduced when the control signal is included in the sliding variable structure. Thus, the problem considered here is to design a robust control based on the available information $\{y, \hat{x}, u\}_{t\ge0}$ such that the so-called UUB-stability of the system (1) is guaranteed in the presence of the external disturbances and uncertain dynamics. Furthermore, the state estimation is designed via the full-order observer (3), and the controller is synthesized in such a way that the state estimation and the available information guarantee the output disturbances mitigation. The controller/observer design combines the concept of the AEM with DSMC theory. Accordingly, after a finite time, the control law drives the system trajectories into a quasi-minimal size attractive ellipsoid and after this time, all trajectories of the system considered arrive to a small positive invariant neighborhood around the origin and remain there.

Proposition 1. (On the attractive set (Poznyak *et al.*, 2014)) *Assume that a real-valued function $V : \mathbb{R}^n \to \mathbb{R}$ satisfies*

$$\frac{\mathrm{d}}{\mathrm{d}t}V(z) \le -\alpha V(z) + \beta, \quad z \in \mathbb{R}^k, \tag{8}$$

for positive scalars α and β. Then $V(z)$ is an attractive set and

$$\limsup_{t\to\infty} V(z) \le \frac{\beta}{\alpha}. \tag{9}$$

Theorem 1. (Attractive-invariant ellipsoid (Poznyak *et al.*, 2014)) *Under the assumption* (8)*, the attractive ellipsoid $\mathcal{E}\left(0, \bar{\mathbf{P}}^{-1}\right)$ is, just as invariant ones, such that the function*

$$G\left(V(z)\right) := \left(\left[V^{\frac{1}{2}}(z) - \sqrt{\frac{\beta}{\alpha}}\right]_+\right)^2,$$

with

$$[\gamma]_+ := \begin{cases}\gamma & \text{if} \quad \gamma \ge 0, \\ 0 & \text{if} \quad \gamma < 0,\end{cases}$$

is the Lyapunov function for the dynamic system (1) having the invariant set

$$\mathcal{D} := \left\{z \in \mathbb{R}^k : G\left(V(z)\right) = 0\right\},$$

and the trajectories satisfy

$$\frac{\mathrm{d}}{\mathrm{d}t}G\left(V\left(z\right)\right)<0 \quad \textit{if} \quad V(z)>\frac{\beta}{\alpha}. \tag{10}$$

Theorem 1 establishes that any trajectory being in or arriving into $\mathcal{D}$ remains inside of this set during all future time. Traditionally, the structure of (8) is obtained from a matrix inequality approach to a control design (Poznyak *et al.*, 2014; Sánchez *et al.*, 2019). As previously mentioned, this is the main reason why the feasibility of the obtained matrix inequality must be guaranteed.

Theorem 2. (On the feasibility of BMI (Gahinet and Pierre, 1994)) *Let* $\boldsymbol{\Psi} \in \mathbb{R}^{h\times h}$ *be a symmetric matrix,* $\boldsymbol{\mathcal{P}} \in \mathbb{R}^{l\times h}$*, and* $\boldsymbol{\mathcal{Q}} \in \mathbb{R}^{k\times h}$ *be matrices such that* $\operatorname{rank}(\boldsymbol{\mathcal{P}}) = r_p < h$, $\operatorname{rank}(\boldsymbol{\mathcal{Q}}) = r_q < h$. *Then the LMI*

$$\boldsymbol{\Psi}+\boldsymbol{\mathcal{P}}^{\intercal}\boldsymbol{\Theta}^{\intercal}\boldsymbol{\mathcal{Q}}+\boldsymbol{\mathcal{Q}}^{\intercal}\boldsymbol{\Theta}\boldsymbol{\mathcal{P}}<0 \tag{11}$$

has a solution $\boldsymbol{\Theta} \in \mathbb{R}^{k\times l}$ *if and only if* $\boldsymbol{\mathcal{W}}_P^{\intercal}\boldsymbol{\Psi}\boldsymbol{\mathcal{W}}_P < 0$ *and* $\boldsymbol{\mathcal{W}}_Q^{\intercal}\boldsymbol{\Psi}\boldsymbol{\mathcal{W}}_Q < 0$*, where* $\boldsymbol{\mathcal{W}}_P$*,* $\boldsymbol{\mathcal{W}}_Q$ *are matrices such that the columns of* $\boldsymbol{\mathcal{W}}_P$ *form a basis of* $\operatorname{kern}(\boldsymbol{\mathcal{P}})$ *and the columns of* $\boldsymbol{\mathcal{W}}_Q$ *form a basis of* $\operatorname{kern}(\boldsymbol{\mathcal{Q}})$ *satisfying* $\boldsymbol{\mathcal{P}}\boldsymbol{\mathcal{W}}_P = \mathbf{0}$, and $\boldsymbol{\mathcal{Q}}\,\boldsymbol{\mathcal{W}}_Q = \mathbf{0}$.

3. Nonlinear robust control design

Consider a manifold $\sigma \in \mathbb{R}^m$, connected with the state estimation space $\hat{x}$ and the control input u, such that

$$\begin{aligned}\sigma &= \begin{bmatrix}\mathbf{K} & \mathbf{I}_{m\times m}\end{bmatrix}\begin{bmatrix}\hat{x}_1\\ \hat{x}_2\\ u\end{bmatrix},\\ \sigma\in\mathbb{R}^m,\quad \mathbf{K} &= \begin{bmatrix}\mathbf{K}_1 & \mathbf{K}_2\end{bmatrix},\end{aligned} \tag{12}$$

where $\mathbf{K}_1 \in \mathbb{R}^{m\times(n-m)}$ and $\mathbf{K}_2 \in \mathbb{R}^{m\times m}$ are fixed gain matrices. Here the sliding variable σ is associated with the storage function $V_1(\sigma(t)) = \frac{1}{2}\sigma^{\intercal}(t)\sigma(t)$.

Proposition 2. (Sliding mode control) *Consider the dynamic system* (1)*, the estimation error* $e = x - \hat{x}$*, and the sliding variable* (12)*. If the control action* u*, under the knowledge of the gain matrices* $\mathbf{K} \in \mathbb{R}^{m\times n}$*,* $\mathbf{L} \in \mathbb{R}^{n\times p}$ *and* $0 < \boldsymbol{\rho} \in \mathbb{R}^{m\times m}$*, has the following dynamics:*

$$\begin{aligned}\dot{u} = -\{&\mathbf{K}_1\left(\mathbf{A}_{11}\hat{x}_1+\mathbf{A}_{12}\hat{x}_2+\mathbf{L}_1\mathbf{C}_1e_1+\mathbf{L}_1\mathbf{C}_2e_2\right)\\ &+\mathbf{K}_2\big(\mathbf{A}_{21}\hat{x}_1+\mathbf{A}_{22}\hat{x}_2+\mathbf{L}_2\mathbf{C}_1e_1\\ &+\mathbf{L}_2\mathbf{C}_2e_2+\mathbf{B}_2u\big)+\boldsymbol{\rho}\,\operatorname{sign}(\sigma(t))\big\},\\ &u(0)=u_0,\quad 0<\boldsymbol{\rho}\in\mathbb{R}^{m\times m},\\ &\delta_1<\lambda_{\min}(\boldsymbol{\rho}):=\delta,\quad \varkappa=\delta-\delta_1,\end{aligned} \tag{13}$$

then the output disturbance bound can be estimated as follows:

$$\begin{aligned}\|\mathbf{K}_5\xi_y\| &= \|\boldsymbol{\rho}\operatorname{sign}(\sigma(t))\|,\\ \mathbf{K}_5 &= \mathbf{K}\mathbf{L}\in\mathbf{R}^{m\times p}.\end{aligned} \tag{14}$$

Moreover, after $t = t_r$ *where* $t_r = \frac{\sqrt{2}}{\varkappa}V_1^{\frac{1}{2}}(\sigma(t_0)) + t_0$*, the hyperplane* $\sigma = 0_m$ *is the sliding manifold for the sliding variable* (12) *and the observer* (3) *has the following form:*

$$\begin{aligned}\dot{\hat{x}} = &\left(\mathbf{A}-\mathbf{B}\mathbf{K}\right)\hat{x}+\mathbf{L}\mathbf{C}e\\ &+\mathbf{L}\mathbf{K}_5^{\intercal}\left(\mathbf{K}_5\mathbf{K}_5^{\intercal}\right)^{-1}\boldsymbol{\rho}\operatorname{sign}(\sigma(t)).\end{aligned} \tag{15}$$

The proof is presented in Appendix (Section A1).

The control approach expressed in (13) is known as DSMC. In this algorithm, the chattering phenomenon is considerably reduced since signal $\dot{u}$ is integrated (Ordaz *et al.*, 2019).

It is worth mentioning that, when the trajectories arrive to the sliding manifold (12), the control structure becomes $u = -\mathbf{K}\hat{x}$.

Note that in the control law (13) the use of error functions e_1 and e_2 does not imply the use of unmeasured state variables, see Remark 1.

Now, by using the output feedback u, the estimation error $e = x - \hat{x}$ and an extended vector $z^{\intercal} = [\hat{x}^{\intercal},\ e^{\intercal}]$,

$$\begin{aligned}\dot{z} &= \boldsymbol{\mathcal{A}}z+\boldsymbol{\mathcal{F}}\bar{\xi}(x,t),\quad z(0)=z_0,\\ \boldsymbol{\mathcal{A}} &:= \begin{bmatrix}\mathbf{A}-\mathbf{B}\mathbf{K} & \mathbf{L}\mathbf{C}\\ \mathbf{0}_{n\times n} & \mathbf{A}-\mathbf{L}\mathbf{C}\end{bmatrix},\\ \boldsymbol{\mathcal{F}} &:= \begin{bmatrix}\mathbf{0}_{n\times n} & \mathbf{L}\\ \mathbf{I}_{n\times n} & -\mathbf{L}\end{bmatrix},\quad \bar{\xi} := \begin{bmatrix}\xi_x(t,x)\\ \xi_y\end{bmatrix}.\end{aligned} \tag{16}$$

It is evident that, for the nominal closed-loop system (16), when the nonlinearities f, uncertain dynamics ζ, and the external disturbances ξ_y are not considered, the eigenvalue spectrum[2] is given by $\bar{\boldsymbol{\sigma}}(\lambda) \subseteq \lambda_i(\mathbf{A}-\mathbf{B}\mathbf{K}) \cup \lambda_i(\mathbf{A}-\mathbf{L}\mathbf{C})$, $i = 1,\ldots,n$, where all the eigenvalues of the controller are decoupled from those of the observer. Thus, it is necessary to stabilize the dynamic system (16). For this purpose, consider the following quadratic function:

$$V_2(z) = z^{\intercal}\mathbf{P}_1z,\quad \mathbf{P}_1 = \begin{bmatrix}\mathbf{P}_2 & \mathbf{0}_{n\times n}\\ \mathbf{0}_{n\times n} & \mathbf{P}_3\end{bmatrix}, \tag{17}$$

with $0 < \mathbf{P}_2 = \mathbf{P}_2^{\intercal}$, $0 < \mathbf{P}_3 = \mathbf{P}_3^{\intercal}$.

Proposition 3. (On the UUB-stability of the closed loop system) *Under the assumption of Proposition 2, if there exists a set of solutions* $(\alpha,\ \varepsilon_1,\ \varepsilon_2\ \mathbf{P},\ \mathbf{K})$*, for the positive*

[2]The eigenvalue spectrum of the extended system $z \in \mathbb{R}^{2n}$ considered is denoted by $\bar{\boldsymbol{\sigma}}(\lambda)$.

scalars α, *and* ε_i *(with* $i = 1, 2$*) such that*

$$\begin{aligned}
\mathbf{W} &= \begin{bmatrix} \mathbf{W}_{11} & \mathbf{P}_2\mathbf{LC} & \mathbf{P}_2\mathbf{L} & \mathbf{0} \\ \mathbf{C}^\intercal\mathbf{L}^\intercal\mathbf{P}_2 & \mathbf{W}_{22} & -\mathbf{P}_3\mathbf{L} & \mathbf{P}_3 \\ \mathbf{L}^\intercal\mathbf{P}_2 & -\mathbf{L}^\intercal\mathbf{P}_3 & -\varepsilon_2\mathbf{I} & \mathbf{0} \\ \mathbf{0} & \mathbf{P}_3 & \mathbf{0} & -\varepsilon_1\mathbf{I} \end{bmatrix} < 0, \\
\mathbf{W}_{11} &= \mathbf{P}_2(\mathbf{A} - \mathbf{BK}) + (\mathbf{A}^\intercal - \mathbf{K}^\intercal\mathbf{B}^\intercal)\mathbf{P}_2 \\
&\quad + \alpha\mathbf{P}_2 + c_2\varepsilon_2\mathbf{I}_n, \\
\mathbf{W}_{22} &= \mathbf{P}_3(\mathbf{A} - \mathbf{LC}) + (\mathbf{A}^\intercal - \mathbf{C}^\intercal\mathbf{L}^\intercal)\mathbf{P}_3 \\
&\quad + \alpha\mathbf{P}_3 + c_2\varepsilon_2\mathbf{I}_n,
\end{aligned} \tag{18}$$

the storage function (17) *satisfies*

$$\lim_{t\to\infty} z^\intercal(t)\bar{\mathbf{P}}_1 z(t) \le 1,\ \bar{\mathbf{P}}_1 = \frac{\alpha}{\beta}\mathbf{P}_1,$$

and the UUB-stability of the system (16) *is concluded, for the parameters*

$$b = \sqrt{\frac{\beta}{\alpha}\lambda_{\max}\mathbf{P}_1^{-1}}$$

and

$$T = \frac{1}{\alpha}\ln\{1 - \frac{\alpha}{\beta}[V_2(z_{t_r}) + \eta]\} + \frac{\sqrt{2}}{\varkappa}V_1^{\frac{1}{2}}(\sigma_0) + t_0,$$

for sufficiently small $\eta \in \mathbb{R}^+$*, where*

$$\begin{aligned}
\beta &:= \varepsilon_1\mu + c_1\varepsilon_2, \\
\mu &:= \lambda_{\max}\left\{\boldsymbol{\rho}^\intercal\left(\mathbf{K}_5\mathbf{K}_5^\intercal\right)^{-\intercal}\boldsymbol{\rho}\right\}.
\end{aligned} \tag{19}$$

The proof is presented in Appendix (Section A2).

Notice that, for $\mathbf{K}_5\mathbf{K}_5^\intercal$ greater than $\boldsymbol{\rho}^\intercal\boldsymbol{\rho}$ (in magnitude terms) and for small enough ε_1, the scalar β is reduced considerably. Thus, $\beta \to c_1\varepsilon_2$, which means that external disturbances on the output are mitigated. Therefore, the controller and observer gain matrices $\mathbf{K}$ and $\mathbf{L}$, respectively, must be high gain matrices. It is remarkable that the control algorithm is valid if and only if the matrix inequality (18) is feasible. The following lemma gives the conditions to guarantee the feasibility of the matrix inequality (18).

Lemma 1. *Consider Theorem 2 and define*

$$\boldsymbol{\Psi} = \begin{bmatrix} \mathbf{W}_{11} & \mathbf{0} & \mathbf{0} & \mathbf{0} \\ \mathbf{0} & \mathbf{W}_{22} & \mathbf{0} & \mathbf{0} \\ \mathbf{0} & \mathbf{0} & -\varepsilon_2\mathbf{I} & \mathbf{0} \\ \mathbf{0} & \mathbf{0} & \mathbf{0} & -\varepsilon_1\mathbf{I} \end{bmatrix}, \tag{20}$$

$$\boldsymbol{\mathcal{P}}^\intercal\boldsymbol{\Theta}^\intercal\boldsymbol{\mathcal{Q}} = \begin{bmatrix} \mathbf{0} & \mathbf{P}_2\mathbf{LC} & \mathbf{P}_2\mathbf{L} & \mathbf{0} \\ \mathbf{0} & \mathbf{0} & -\mathbf{P}_3\mathbf{L} & \mathbf{P}_3 \\ \mathbf{0} & \mathbf{0} & \mathbf{0} & \mathbf{0} \\ \mathbf{0} & \mathbf{0} & \mathbf{0} & \mathbf{0} \end{bmatrix},$$

where

$$\boldsymbol{\mathcal{P}} = \begin{bmatrix} \mathbf{P}_2 & \mathbf{0} & \mathbf{0} & \mathbf{0} \\ \mathbf{0} & \mathbf{I} & \mathbf{0} & \mathbf{0} \end{bmatrix},$$

$$\boldsymbol{\mathcal{Q}} = \begin{bmatrix} \mathbf{0} & -\mathbf{LC} & \mathbf{L} & \mathbf{0} \\ \mathbf{0} & \mathbf{0} & \mathbf{P}_3\mathbf{L} & -\mathbf{P}_3 \end{bmatrix},$$

$$\boldsymbol{\Theta} = \mathbf{I},$$

with their respective associated kernels

$$\boldsymbol{\mathcal{W}}_P = \begin{bmatrix} \mathbf{0} & \mathbf{0} & \mathbf{I} & \mathbf{0} \\ \mathbf{0} & \mathbf{0} & \mathbf{0} & \mathbf{I} \end{bmatrix}^\intercal,$$

$$\boldsymbol{\mathcal{W}}_Q = \begin{bmatrix} \mathbf{0} & \mathbf{I} & \mathbf{C} & \mathbf{LC} \\ \mathbf{I} & \mathbf{0} & \mathbf{0} & \mathbf{0} \end{bmatrix}^\intercal.$$

Then the matrix inequality (18) *takes the form* (11) *and the feasibility of* $\mathbf{W}$ *is guaranteed.*

From the previous lemma, it is evident that

$$\begin{aligned}
&\boldsymbol{\mathcal{W}}_Q^\intercal\boldsymbol{\Psi}\boldsymbol{\mathcal{W}}_Q \\
&= \begin{bmatrix} \mathbf{W}_{11} & \mathbf{0}_{n\times n} \\ \mathbf{0}_{n\times n} & \mathbf{W}_{22} - \varepsilon_2\mathbf{C}^\intercal\mathbf{C} - \varepsilon_1\mathbf{C}^\intercal\mathbf{L}^\intercal\mathbf{LC} \end{bmatrix} < 0.
\end{aligned} \tag{21}$$

This property indicates that the separation principle in linear systems for a full-order controller/observer scheme is achieved.

4. Small size ultimate bound

To obtain a solution in terms of a quasi-minimal attractive ellipsoid, it is necessary to solve the BMI (18). The most common tool to achieve a matrix inequality solution is by using a matrix transformation to obtain a constrained LMI problem (Poznyak *et al.*, 2014). The next lemma presents an isomorphic LMI related to (18).

Proposition 4. (On the LMI transformation) *If the set of linear matrix inequalities*

$$\begin{aligned}
0 < &\begin{bmatrix} \mathbf{BY}_1 + \mathbf{Y}_1^\intercal\mathbf{B}^\intercal - \mathbf{A}^\intercal\mathbf{X} - \mathbf{AX1} - \alpha\mathbf{X} & \mathbf{I} & \mathbf{X} \\ \mathbf{I} & \mathbf{X} & \\ \mathbf{Q} & \mathbf{0}_{n\times n} & \\ \mathbf{0}_{n\times n} & \frac{1}{c_2\varepsilon_2}\mathbf{I}_n & \end{bmatrix}, \\
&0 < \mathbf{X} \in \mathbb{R}^{n\times n}, \quad 0 < \mathbf{Q} \in \mathbb{R}^{n\times n}, \quad \mathbf{Y}_1 \in \mathbb{R}^{m\times n}
\end{aligned} \tag{22}$$

and

$$0 < \begin{bmatrix} \mathbf{R} \\ -\mathbf{C}^\intercal\mathbf{Y}_2^\intercal \\ \mathbf{Y}_2^\intercal \\ \mathbf{0}_{n\times n} \end{bmatrix} \begin{matrix} -\mathbf{Y}_2\mathbf{C} \\ \mathbf{Y}_2\mathbf{C} + \mathbf{C}^\intercal\mathbf{Y}_2^\intercal - \mathbf{P}_3\mathbf{A} - \mathbf{A}^\intercal\mathbf{P}_3 - \alpha\mathbf{P}_3, \\ -\mathbf{Y}_2^\intercal \\ -\mathbf{P}_3 \end{matrix} \begin{bmatrix} \mathbf{Y}_2 & \mathbf{0}_{n\times n} \\ -\mathbf{Y}_2 & -\mathbf{P}_3 \\ \varepsilon_2\mathbf{I}_p & \mathbf{0}_{p\times n} \\ \mathbf{0}_{n\times p} & \varepsilon_1\mathbf{I}_n \end{bmatrix},$$
$$0 < \mathbf{R} + \mathbf{Q} - 2\mathbf{P}_3, \quad (0 < \mathbf{P}_3, \quad 0 < \mathbf{R}) \in \mathbb{R}^{n\times n},$$
$$\mathbf{Y}_2 \in \mathbb{R}^{n\times p}, \tag{23}$$

holds for positive scalars ε_1, ε_2 and α, then the matrix inequality (18) *is fulfilled.*

The proof is presented in Appendix (Section A3).

In addition to (22) and (23), the following constraint:

$$\begin{bmatrix} \mathbf{M} & \mathbf{I} \\ \mathbf{I} & \mathbf{P}_3 \end{bmatrix} > 0 \tag{24}$$

is introduced, which is equivalent to $\mathbf{M} > \mathbf{P}_3^{-1}$. Then, the problem can be expressed as an approximated solution of the following constrained optimization problem:

$$\min_{\mathbf{P}^{-1}} \left(\frac{\beta}{\alpha} \text{trace}\left\{\mathbf{P}^{-1}\right\} \right), \tag{25}$$

subject to (22), (23), (24) and $0 < \mathbf{P}_1, \quad 0 < \varepsilon_1, \quad 0 < \varepsilon_2, \quad 0 < \alpha$.

If there exists a solution set ($\mathbf{X}$, $\mathbf{P}_3$, $\mathbf{Q}$, $\mathbf{R}$, $\mathbf{Y}_1$, $\mathbf{Y}_2$, $\mathbf{M}$, α, ε_1, ε_2) such that the previous optimization problem holds, then Proposition 1 holds, too. This means that the ellipsoid $\mathcal{E}(0, \bar{\mathbf{P}}^{-1})$ is attractive and at the same time invariant; see Theorem 1. According to Proposition 2, after time $t_r = \frac{\sqrt{2}}{\varkappa} V_1^{\frac{1}{2}}(\sigma(t_0)) + t_0$, the trajectory arrives to an ultimate bound in exponential form. The arriving rate is given by α; see, for instance, Eqn. (8) of Proposition 1 or the proof of Proposition 3 in Appendix (Section A2). Additionally, by decreasing the parameters ε_1 and ε_2, the effects of external disturbances and uncertain dynamics are reduced.

In Algorithm 1, the ultimate bound is computed. In a numerical sense, this algorithm produces the best solution set to conclude the UUB-stability of the system (16), with a small size ultimate bound b associated with a quasi-minimal invariant-attractive ellipsoid $\mathcal{E}(0, \bar{\mathbf{P}}^{-1})$.

Algorithm 1. Ultimate bound numerical computation.

(i) Considering $i = 0$, set the initial scalar parameters α, ε_1 and ε_2 as α_0, $\varepsilon_{1,0}$ and $\varepsilon_{2,0}$, respectively. In this step, propose a small value of α_0 and large values of $\varepsilon_{1,0}$, $\varepsilon_{2,0}$.

(ii) Use some LMI solver tool, and find a solution to the constrained optimization problem (25).

(iii) While the LMI has a solution, do:

- **(a)** Update the index i to $i = i + 1$, and modify the parameters $\varepsilon_{1,i}$ and $\varepsilon_{2,i}$ as follows $\varepsilon_{1,i} = \varepsilon_{1,i-1} - \Delta\varepsilon_{1,i}$, $0 < \Delta\varepsilon_{1,i} \ll 1$, $\varepsilon_{2,i} = \varepsilon_{2,i-1} - \Delta\varepsilon_{2,i}$, $0 < \Delta\varepsilon_{2,i} \ll 1$.
- **(b)** If the solution of (25) holds with $\varepsilon_{1,i}$ and $\varepsilon_{2,i}$, save this solution, as $\mathbf{X}_0$, $\mathbf{P}_{3,0}$, $\mathbf{Q}_0$, $\mathbf{R}_0$, $\mathbf{Y}_{1,0}$, $\mathbf{Y}_{2,0}$, $\mathbf{M}_0$, α_0, $\varepsilon_{1,0}$, $\varepsilon_{2,0}$, and return to **(a)**.
- **(c)** If there is no solution, terminate Step **(iii)**.

(iv) Resetting $i = 0$, and using the last admissible parameters α_0, $\varepsilon_{1,0}$ and $\varepsilon_{2,0}$, once again, it is necessary to find an updated solution of the constrained optimization problem (25), doing:

- **(a)** Update the index i to $i = i + 1$, and increase the parameter α_i as $\alpha_i = \alpha_{i-1} + \Delta\alpha$, $0 < \Delta\alpha \ll 1$, such that the inequalities (25) holds.
- **(b)** If the solution of (25) holds, save this as **(b)** of **(iii)**.
- **(c)** Otherwise, stop this iterative parameter update, and terminate **(iv)**.

(v) The last admissible parameters $\mathbf{X}_0, = \mathbf{X}_0^*$, $\mathbf{P}_{3,0} = \mathbf{P}_{3,0}^*$, $\mathbf{Q}_0, = \mathbf{Q}_0,^*$ $\mathbf{R}_0 = \mathbf{R}_0^*$, $\mathbf{Y}_{1,0} = \mathbf{Y}_{1,0}^*$, $\mathbf{Y}_{2,0} = \mathbf{Y}_{2,0}^*$, $\mathbf{M}_0 = \mathbf{M}_0^*$, $\alpha_0 = \alpha_0^*$, $\varepsilon_{1,0} = \varepsilon_{1,0}^*$, $\varepsilon_{2,0} = \varepsilon_{2,0}^*$. are declared as the best iterative solution.

(vi) Finally, the controller/observer gain matrices are defined as $\mathbf{K} = \mathbf{Y}_{1,0}\mathbf{X}_0^{-1}$, and $\mathbf{L} = \mathbf{P}_{3,0}^{-1}\mathbf{Y}_{2,0}$. Also, under the assumption of (9), the ultimate bound is declared as

$$b = \sqrt{\frac{\varepsilon_{1,0}\mu_0 + c_1\varepsilon_{2,0}}{\alpha} \max(\lambda_{\max}\mathbf{P}_{2,0}^{-1}, \lambda_{\max}\mathbf{P}_{3,0}^{-1})}.$$

5. Illustrative example

In order to validate the theoretical results previously presented in this work, a numerical example dealing with a double mass spring damper system driven by DC-motor is considered. The use of DC-motors for validating control algorithms is a common practice among researchers (see, e.g., Luna *et al.*, 2020; Khalil and

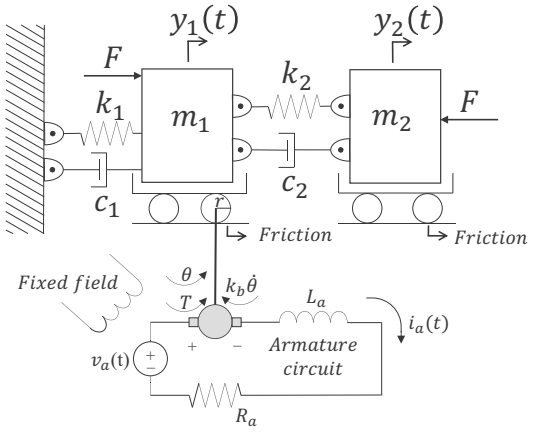

Fig. 1. Electromechanical system.

Table 1. Parameters of the double mass spring damper system driven by a DC-motor.

Description	Notation	Value	Units
Mass 1	m_1	0.52	kg
Mass 2	m_2	0.23	kg
Stiffness of the spring 1	k_1	0.0923	$\frac{\text{N}}{\text{m}}$
Stiffness of the spring 2	k_2	0.103	$\frac{\text{N}}{\text{m}}$
Damping coefficient 1	c_1	0.203	$\text{N}\frac{\text{s}}{\text{m}}$
Damping coefficient 2	c_2	0.197	$\text{N}\frac{\text{s}}{\text{m}}$
Armature inductance	L_a	0.0218	mH
Motor-torque constant	k_a	0.767	$\frac{\text{N}\cdot\text{m}}{\text{A}}$
Armature resistance	R_a	1.3	Ohm
Back-EMF constant	k_b	0.767	$\frac{\text{V}\cdot\text{s}}{\text{rad}}$
Wheel ratio	r	0.0051	m

Elshenawy, 2021).

5.1. Servomechanism system. A simplified schematic diagram of the single-input multiple-output system considered is shown in Fig. 1. The control challenge for this system is to move the second mass to a desired set-point or trajectory by controlling the first mass, which is driven by the armature voltage $v(t)$ of the DC-motor. Furthermore, the system output is defined by position measurements, y_1 and y_2, leaving the velocities $\dot{y}_1$ and $\dot{y}_2$ corresponding to each mass, and the armature current i_a to be estimated.

Therefore, the system variables considered are defined as $x_1^\intercal = \begin{bmatrix} y_1 & \dot{y}_1 & y_2 & \dot{y}_2 \end{bmatrix}^\intercal \in \mathbb{R}^4$, $x_2 = i \in \mathbb{R}$, and the system input is associated as $u = v_a \in \mathbb{R}$. Thus, the mathematical model of the double mass spring damper system driven by a DC-motor can be expressed as five-dimensional first-order differential equations of the type (1), where the associated nominal system is given by

$$\begin{aligned}
\mathbf{A}_{11} &= \begin{bmatrix} 0 & 1 & 0 & 0 \\ -\frac{k_1+k_2}{m_1} & -\frac{b_1+b_2}{m_1} & \frac{k_2}{m_1} & \frac{b_2}{m_1} \\ 0 & 0 & 0 & 1 \\ \frac{k_2}{m_2} & \frac{b_2}{m_2} & -\frac{k_2}{m_2} & -\frac{b_2}{m_2} \end{bmatrix}, \\
\mathbf{A}_{12} &= \begin{bmatrix} 0 \\ \frac{k_b}{m_1} \\ 0 \\ 0 \end{bmatrix}, \\
\mathbf{A}_{21} &= \begin{bmatrix} 0 & 0 & 0 - \frac{k_a}{L_a}\pi r^2 \end{bmatrix}, \\
\mathbf{A}_{22} &= -\frac{R_a}{L_a}, \\
\mathbf{B}_1 &= \bar{0}_4, \quad \mathbf{B}_2 = \frac{1}{L_a}, \\
\mathbf{C} &= \begin{bmatrix} 1 & 0 & 0 & 0 & 0 \\ 0 & 0 & 1 & 0 & 0 \end{bmatrix}.
\end{aligned} \tag{26}$$

The parameter k_a is the motor-torque constant; in general, this constant is the same as the back electromotive force (back-emf) constant, i.e., in magnitude $k_b = k_a$. The armature resistance is denoted by R_a, and L_a is the armature inductance, both being positive. All the system parameters are given in Table 1. For this single-input multiple-output system, it is evident that pairs $(\mathbf{A}, \mathbf{B})$ and $(\mathbf{C}, \mathbf{A})$ are controllable and observable, respectively. The system trajectories are disturbed by the vector $\xi_x(x,t)$, which is assumed to be bounded. This assumption is supported by the friction phenomena acting on each mass displacement. The vast majority of mathematical models for friction effects are strongly nonlinear (Ruderman, 2015; Rudenko and Hedberg, 2013). This dynamic feature is considered in $\xi_x(t,x)$, and it can be bounded as the first part of (2).

Nowadays, the friction models are studied in the tribology field, where the model synthesis is done considering traditional viscous and Coulomb friction effects, or also complex ones like Armstrong, Lugre and Maxwell-slip formalisms (Ruderman, 2015). Furthermore, the external disturbances $\xi_y(t,x)$ are associated with each mass displacement, and, as was previously mentioned, they are assumed to be bounded. In this numerical test, the disturbances and system uncertainties related to $\xi_x(t,x)$ are considered as

$$\begin{aligned}
\xi_x(t,x) &= \begin{bmatrix} 0 & \xi_{x,2} & 0 & \xi_{x,4} & 0 \end{bmatrix}^\intercal, \\
\xi_{x,2} &= -0.002x_2 - 0.00041\text{sign}(x_2) \\
&\quad - 0.2^2 k_1 x_1^3 - 0.18^2 k_2 (x_1 - x_2)^3, \\
\xi_{x,4} &= -0.0021x_4 - 0.00241\text{sign}(x_4) \\
&\quad - 0.18^2 k_2 (x_2 - x_1)^3.
\end{aligned} \tag{27}$$

The uncertain dynamic $\xi_x(t,x)$ is taken from the classical Viscous and Coulomb friction models; moreover, this uncertainty contains nonlinear dynamics of the spring

restoring force. Furthermore, another disturbance is considered in the system output:

$$\xi_y(t,x)=\begin{bmatrix}0.012+0.12\sin(12t)+\psi_{y_1}(t),\\ 0.017+0.23\sin(22t)+\psi_{y_2}(t)\end{bmatrix}. \quad (28)$$

The other parts, $\psi_{y_1}(t,x) = 0.05H_{t_{10}} - 0.05H_{t_{10.4}}$ and $\psi_{y_2}(t,x) = 0.066H_{t_{14}} - 0.065H_{t_{14.4}}$, were introduced at two different time intervals $t_{p_1}\in[10, 10.4]$ and $t_{p_2}\in[14, 14.4]$ s, respectively. Here H_{t_s} is the well-known Heaviside step function, defined by

$$H_{t_s}:=\begin{cases}1 & \text{if} \quad t_s\geq 0,\\ 0 & \text{if} \quad t_s<0.\end{cases}$$

To assess the effectiveness of the proposed control algorithm, a comparative study with alternative schemes is conducted. Firstly, a state-feedback sliding mode control (SF-SMC) with a Luenberger-type full state observer is designed. Secondly, a control algorithm based on the linear quadratic regulator (*LQR*), where the unmeasured state variables were estimated using an SMO, is considered. Next, by following the iterative algorithm presented in Section 4, the controller and observer parameters of the proposed scheme are obtained. Finally, using pole allocation to tune the traditional controller/observer approach is discussed. It is worth mentioning that, in each case, the controller/observer gains are computed such that a fair comparative study is achieved. This does not imply that there is not a set of gains that can yield a better performance.

5.2. Sliding mode control with a full order observer. For this approach, assume that the system is free from uncertain dynamics, nonlinearities, and external disturbances. The nominal linear system is

$$\dot{x}=\mathbf{A}x+\mathbf{B}u, \quad x(0)=x_0, \quad y=\mathbf{C}x. \quad (29)$$

Therefore, a full order observer in the form of (3) is designed. In this way, the state estimate error function is considered as $e = x - \hat{x}$, which means that the error dynamics are

$$\dot{e}=(\mathbf{A}-\mathbf{LC})e. \quad (30)$$

To ensure that the error function asymptotically converges to the trivial solution, the matrix $(\mathbf{A} - \mathbf{LC})$ needs to be Hurwitz. Thus, the observer matrix

$$\mathbf{L}=\begin{bmatrix}3.6917 & -0.0172\\ 1.0646 & -0.4201\\ -0.0172 & 3.2699\\ 0.3003 & 0.8463\\ -0.2880 & -0.9510\end{bmatrix} \quad (31)$$

allocates the observer eigenvalues at $\lambda_i = \{-68.8403, -1.5338 \pm 1.6184j, -2.9838 \pm 0.1920j\}$, with $j^2 = -1$. After the observer design, consider the SF-SMC as reported by Shtessel *et al.* (2014). To this end, consider the following control action:

$$\mathbf{u}(t)=\boldsymbol{K}_{\text{smc}}\text{sign}(\sigma), \quad \boldsymbol{K}_{\text{smc}}=[\boldsymbol{K}_{\text{pp}},\ 1], \quad (32)$$

where the sliding manifold is given by $\sigma = [\boldsymbol{K}_{\text{smc}},\ 1]\hat{x}$ (in this case, the state estimate $\hat{x}$ is considered). After the tuning procedure via pole allocation, the following gain is obtained:

$$\boldsymbol{K}_{\text{smc}}=\big[-0.0218\ \ 0.0249\ \ -0.0087 \\ -1.5739\ \ -1.2470\big]. \quad (33)$$

Finally, to attenuate the chattering effect of this control scheme, the equivalent control is estimated via low-pass filtering as follows:

$$\begin{aligned}\mathbf{u}_{\text{eq}}(t)&=-\boldsymbol{K}_{\text{slidg}}\hat{x}-7\psi(t),\\ \dot{\psi}(t)&=-\frac{\psi(t)+\text{sign}(\sigma)}{h},\\ \boldsymbol{K}_{\text{slidg}}&=\boldsymbol{K}_{\text{smc}}\mathbf{A}_{11}/\mathbf{B}_2, \quad h=0.01.\end{aligned} \quad (34)$$

5.3. Linear quadratic regulator with a sliding mode observer. As presented in the former scheme, the controller/observer algorithm is designed for system (29) under transformation $\bar{x} = \mathbf{\Gamma}\hat{x}$. The observer was designed by following the procedure given by Sánchez *et al.* (2019). In this way, the SMO is synthesized as

$$\dot{\bar{x}}=\mathcal{A}\bar{x}+\mathcal{B}u+\mathcal{L}\phi(e_2), \quad \bar{x}(0)=\mathbf{\Gamma}\bar{x}_0, \quad (35)$$

with

$$\mathcal{L}=\begin{bmatrix}\mathbf{L}_1\\ \boldsymbol{I}_p\end{bmatrix}, \quad \phi(e_2)=\mathcal{A}_{22}e_2+\mathbf{R}_s\text{sign}(e_2). \quad (36)$$

After the tuning procedure, the following observer gains are achieved:

$$\begin{aligned}\mathbf{L}_1&=\begin{bmatrix}-1.5712 & 0.3528\\ -0.3528 & 1.7425\\ 0.4079 & -1.8067\end{bmatrix},\\ \mathbf{R}_s&=\begin{bmatrix}1.3 & 0\\ 0 & 1.21\end{bmatrix}.\end{aligned} \quad (37)$$

Then, the LQR was used to compute the control law where the weighting matrices are the following:

$$\begin{aligned}\mathbf{Q}_{\text{lqr}}&=\text{diag}(\big[2.99,\ 2.6,\ 3.25,\\ &\qquad 2.34,\ 2.99,\ 3.51\big]),\\ \mathbf{R}_{\text{lqr}}&=1.2,\end{aligned} \quad (38)$$

which leads to the control gain

$$\mathbf{K}_{\text{lqr}}=\big[1.0661\ \ 1.4856\ \ 0.9630 \\ 0.4394\ \ 0.7129\big]. \quad (39)$$

5.4. Proposed controller/observer scheme. The numerical solution of the iterative algorithm based on Proposition 4, presented in Section 4, is implemented in MATLAB via the YALMIP/SeDuMi Toolbox. After applying the numerical algorithm, an approximation of the solution of the optimization problem (25) is obtained, and it has the following numerical values:

$$\mathbf{K} = \begin{bmatrix} 5.4412 & 7.2827 & 0.3289 & 17.9521 & 1.8720 \end{bmatrix},$$

$$\mathbf{L} = \begin{bmatrix} 128.2573 & -98.0199 \\ 208.9008 & -198.5837 \\ -46.1011 & 79.4384 \\ -138.3495 & 138.9273 \\ 84.9406 & -76.8294 \end{bmatrix} \times 10^2 \tag{40}$$

for the positive-definite matrices

$$\mathbf{P}_2 = \begin{bmatrix} 0.0467 & 0.0143 & 0.0043 \\ 0.0143 & 0.0191 & 0.0009 \\ 0.0043 & 0.0009 & 0.1272 \\ 0.1614 & 0.0484 & 0.1987 \\ 0.0000 & 0.0000 & 0.0000 \end{bmatrix} \begin{bmatrix} 0.1614 & 0.0000 \\ 0.0484 & 0.0000 \\ 0.1987 & 0.0000 \\ 2.6928 & 0.0000 \\ 0.0000 & 0.0001 \end{bmatrix} \times 10^2,$$

$$\mathbf{P}_3 = \begin{bmatrix} 0.0005 & -0.0002 & 0.0001 \\ -0.0002 & 0.0003 & -0.0000 \\ 0.0001 & -0.0000 & 0.0005 \\ -0.0001 & 0.0002 & 0.0000 \\ -0.0001 & -0.0001 & 0.0002 \end{bmatrix} \begin{bmatrix} -0.0001 & -0.0001 \\ 0.0002 & -0.0001 \\ 0.0000 & 0.0002 \\ 0.1785 & 0.3022 \\ 0.3022 & 0.5126 \end{bmatrix} \times 10^3, \tag{41}$$

and the additional matrices

$$\mathbf{Q} = \begin{bmatrix} 7.0632 & -0.0838 & 0.0036 \\ -0.0838 & 7.1007 & -0.0358 \\ 0.0036 & -0.0358 & 6.9795 \\ -0.0725 & 0.0266 & -0.0545 \\ -0.0125 & 0.0485 & 0.0574 \end{bmatrix} \begin{bmatrix} -0.0725 & -0.0125 \\ 0.0266 & 0.0485 \\ -0.0545 & 0.0574 \\ 7.1237 & 0.0300 \\ 0.0300 & 7.1721 \end{bmatrix} \times 10^4,$$

$$\mathbf{R} = \begin{bmatrix} 0.9344 & 0.0140 & -0.0443 \\ 0.0140 & 0.9153 & 0.0281 \\ -0.0443 & 0.0281 & 1.0112 \\ 0.0531 & 0.0357 & -0.0159 \\ 0.0136 & -0.0606 & -0.0695 \end{bmatrix} \begin{bmatrix} 0.0531 & 0.0136 \\ 0.0357 & -0.0606 \\ -0.0159 & -0.0695 \\ 0.8905 & -0.0371 \\ -0.0371 & 0.8401 \end{bmatrix} \times 10^5, \tag{42}$$

with the scalar parameters $\alpha = 0.25$, $\varepsilon_1 = 0.0006$, $\varepsilon_2 = 0.012$, $\mu = 0.0016$, $c_1 = 0.012$ and the output disturbance bound $\|\xi_y(t,x)\| \leq 0.0088$.

5.5. Linear controller with a full order Luenberger type observer. The observer used for this scheme is the same as that designed in Section 5.2. Hence the full order observer of the system (29) is given by (30), under the same observation gain (31). At this point, consider the linear feedback $u = -\boldsymbol{K}\hat{x}$ via Ackermann's algorithm, where the desired closed-loop system poles were placed at $\lambda_i = \{-149.18, -3.86, -0.87, -0.63 \pm 0.43j\}$.

5.6. Numerical results. The numerical test was implemented in MATLAB-Simulink R2016a, under the 4th order Runge–Kutta ODE solver with a fixed step $h_p = 0.001$ s. The considered simulation time belongs to the time interval $t \in [0, 50]$ s. The initial conditions, of the electromechanical system were assigned as

$$x_0 = [0.4,\ 0.05\,0.2\ -0.07\,0]^{\mathsf{T}},$$

$$\hat{x}_0 = [0\ 0\ 0\ 0\ 0]^{\mathsf{T}}, \quad u_0 = 0.$$

Table 2 presents the nomenclature used to represent each controller/observer scheme 2–6. The real system positions $y_1(t) - y_2(t)$ and the estimated positions are depicted in Fig. 2, which contains a zoom of this estimation. Moreover, Fig. 3 shows the system velocity estimates $\dot{y}_1$ and $\dot{y}_2$. The armature current and the armature voltage are plotted in Fig. 4. Notice that Fig. 4 shows signals resembling noise however, this effect is not noise, it is given by a chattering phenomenon not entirely avoided by the controller design. They are present although DSMC reduces considerably the chattering effect. The reduction in this effect given in $\dot{u}$

Table 2. Nomenclature of Figs. 2–6.

Description	Controller/observer scheme
Method 1	SF-SMC + full order observer
Method 2	LQR + SMO
Method 3	Proposed controller/observer
Method 4	Full order controller/observer

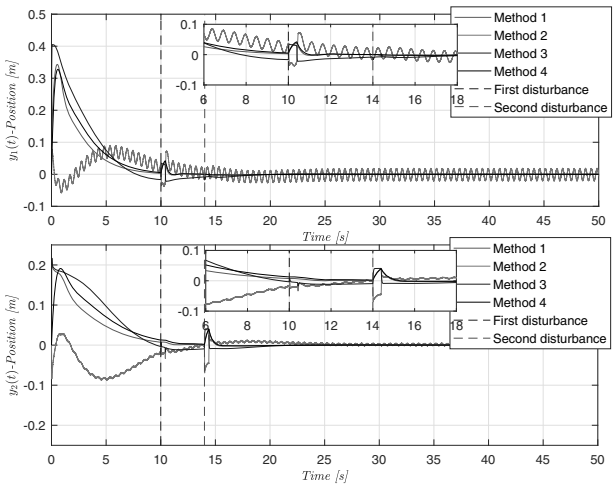

Fig. 2. Estimated positions $y_1(t)$ and $y_2(t)$.

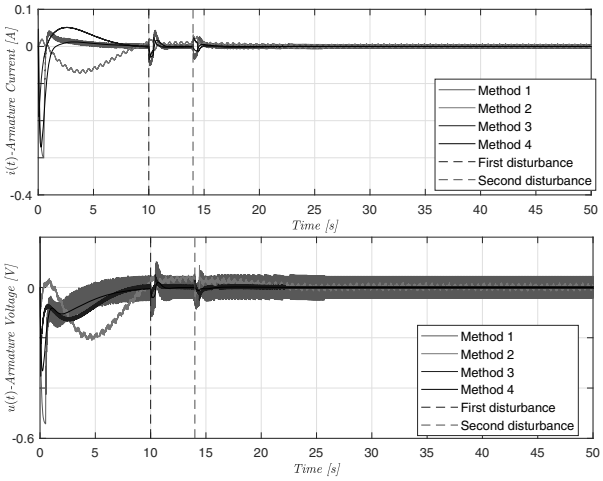

Fig. 4. Armature current and voltage, $i_a(t)$ and $V_a(t)$, respectively.

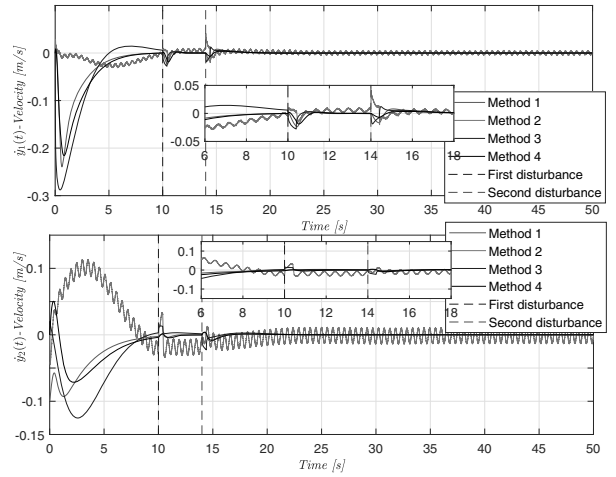

Fig. 3. Estimated velocities $\dot{y}_1(t)$ and $\dot{y}_2(t)$.

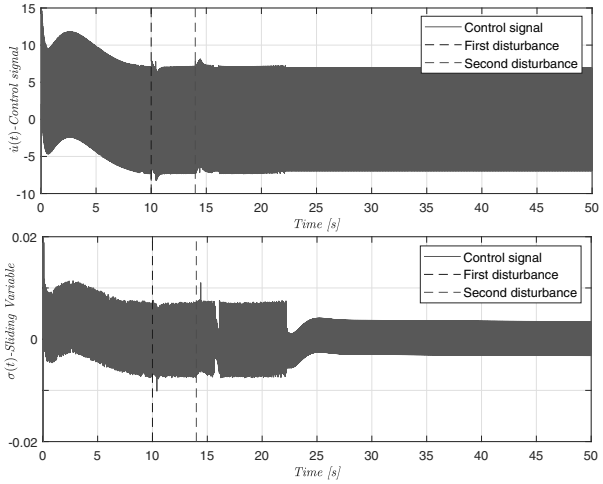

Fig. 5. Proposed control signal and its sliding surface.

is depicted in Fig. 5. Actually, this noisy like effect is given by the viscous friction effects. The control signal $\dot{u}$ and the sliding variable are depicted in Fig. 5, which shows how the variable σ attains the sliding manifold in finite time $t = 4.201$ s. Finally, the sliding surfaces of the SMC and SMO are shown in Fig. 6.

It is remarkable that, after the time $t \geq 4.201$ s, the system trajectories go around the trivial solution $\hat{x}(t) = \bar{0}_5$, in exponential form. This because

$$\begin{aligned} \text{trace}\{\mathbf{P}^{-1}\} &= 2.8858 \times 10^3, \\ \lambda_{\min}(\mathbf{P}^{-1}) &= 1.8031 \times 10^{-9}, \\ \lambda_{\max}(\mathbf{P}^{-1}) &= 2.7187 \times 10^3, \\ \frac{\beta}{\alpha} &= 1.0992 \times 10^{-6}, \end{aligned}$$

thus

$$\sqrt{\frac{\beta}{\alpha}\lambda_{\max}\mathbf{P}^{-1}} \leq 0.00301.$$

Moreover T=8.23 s. To support the effectiveness of the output control strategy proposed here, the integral absolute error (IAE), the integral time absolute error (ITAE), the integral square error (ISE) and the integral time square error (ITSE) criteria of the proposed controller/observer versus others schemes are shown in Table 3. In this paper, which is based on numerical simulation, the error function can directly be computed as $e = x - \hat{x}$.[3] Furthermore, an energy analysis was made

[3]The error analysis is given for the square error and the absolute error defined as $\|e\|^2 = e^\intercal e$ and $\|e\| = (e^\intercal e)^{\frac{1}{2}}$, respectively.

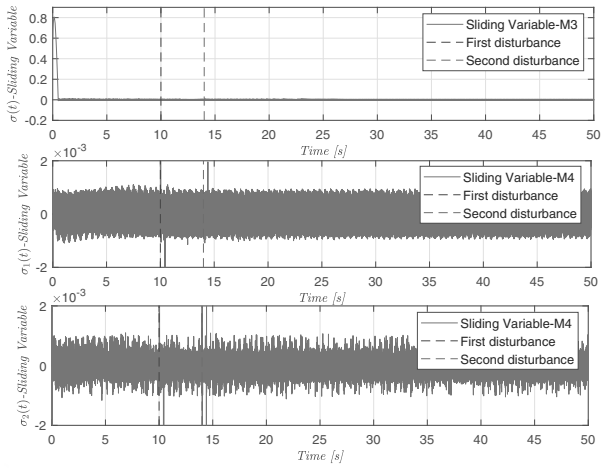

Fig. 6. Sliding surfaces.

Table 3. Error analysis of the servomechanism system.

Scheme	ISE	IAE	ITAE	ITSE
Method 1	1.0253	4.4851	50.6411	0.0250
Method 2	0.0426	1.1056	22.4117	0.0069
Method 3	1.5940	0.1344	23.8746	0.0068
Method 4	0.0685	1.2113	22.5705	0.0071

by considering another function:

$$E_T = \int_0^t \mathbf{u}(\tau)^\intercal \mathbf{u}(\tau)\, \mathrm{d}s. \tag{43}$$

In this way, the energy of the control signal produces the following results:

$$E_{T_{M1}} = 2.7214\ \mathrm{V}^2 \cdot \mathrm{s},$$

$$E_{T_{M2}} = 0.2109\ \mathrm{V}^2 \cdot \mathrm{s},$$

$$E_{T_{M3}} = 0.1327\ \mathrm{V}^2 \cdot \mathrm{s},$$

$$E_{T_{M4}} = 0.2639\ \mathrm{V}^2 \cdot \mathrm{s}.$$

Note that, for the ISE criterion, the scheme that had the best performance corresponds to Method 2, for the IAE to the Method 3, for the ITAE the Method 2, and for the ITSE to the Method 3. In energy consumption terms, the algorithm with the best performance is the scheme Method 3. Thus, for this comparative study, the scheme with the best performance is the proposed controller/observer algorithm.

6. Conclusion

In this paper, the DSMC and AEM theories were combined in order to obtain a UUB-Stable controller/observer algorithm. The designed control scheme implies effective state estimation by using a full-order observer, where the disturbed system considered includes external disturbances, unknown uncertainties, and/or non-modeled dynamics. Since the design procedure is an extension of the conventional AEM, it incorporates an auxiliary nonlinear optimization problem, where the feasibility of the matrix inequalities is guaranteed, and therefore, it assures that the separation principle, for the controller/observer algorithm considered, is fulfilled for this class of systems. Furthermore, a numerical procedure to reduce the ultimate bound was presented, and the time to arrive to this invariant set was estimated as

$$T = \frac{1}{\alpha}\ln\{1-\frac{\alpha}{\beta}\left[V_2(z_{t_r})+\eta\right]\} + \frac{\sqrt{2}}{\varkappa}V_1^{\frac{1}{2}}(\sigma_0) + t_0,$$

where t_r was given in Proposition 2 and estimated using (14). Finally, to validate the theoretical results, the control approach was tested on a benchmark electromechanical system, producing a successful system behavior.

References

Andrade-Da Silva, J.M., Edwards, C. and Spurgeon, S.K. (2009). Linear matrix inequality based dynamic output feedback sliding mode control for uncertain plants, *American Control Conference, ACC'09, St. Louis, USA*, pp. 763–768.

Atassi, A.N. and Khalil, H.K. (1999). A separation principle for the stabilization of a class of nonlinear systems, *IEEE Transactions on Automatic Control* **44**(9): 1672–1687.

Cao, K., Qian, C. and Gu, J. (2023). Global sampled-data stabilization via static output feedback for a class of nonlinear uncertain systems, *International Journal of Robust and Nonlinear Control* **33**(4): 2913–2929.

Choi, H.H. and Ro, K. (2005). LMI-based sliding-mode observer design method, *IEE Proceedings: Control Theory and Applications* **152**(1): 113–115.

Gahinet, P. and Pierre, A. (1994). A linear matrix inequality approach to H^∞ control, *International Journal of Robust and Nonlinear Control* **4**(4): 421–448.

Haddad, W.M. and Chellaboina, V. (2011). *Nonlinear Dynamical Systems and Control: A Lyapunov-based Approach*, Princeton University Press, Princeton.

Jafari, M. and Mobayen, S. (2019). Second-order sliding set design for a class of uncertain nonlinear systems with disturbances: An LMI approach, *Mathematics and Computers in Simulation* **156**: 110–125, DOI: 10.1016/j.matcom.2018.06.015.

Khalil, K.M. and Elshenawy, A. (2021). Robust model integral predictive control design for reference tracking dc servomechanism, *2021 10th International Conference on Intelligent Computing and Information Systems (ICICIS), Cairo, Egypt*, pp. 243–253.

Kukurowski, N., Mrugalski, M., Pazera, M. and Witczak, M. (2022). Fault-tolerant tracking control for a non-linear twin-rotor system under ellipsoidal bounding, *International Journal of Applied Mathematics and Computer Science* **32**(2): 171–183, DOI: 10.34768/amcs-2022-0013.

Liu, H. and Khalil, H.K. (2019). Output feedback stabilization using super-twisting control and high-gain observer, *International Journal of Robust and Nonlinear Control* **29**(3): 601–617.

Luna, L., Asiain, E. and Garrido, R. (2020). Servo velocity control using a p+ ADOB controller, *IFAC-PapersOnLine* **53**(2): 1300–1305.

Ordaz, P., Ordaz, M., Cuvas, C. and Santos, O. (2019). Reduction of matched and unmatched uncertainties for a class of nonlinear perturbed systems via robust control, *International Journal of Robust and Nonlinear Control* **29**(8): 2510–2524.

Peng, C., Zhang, A. and Li, J. (2021). Neuro-adaptive cooperative control for high-order nonlinear multi-agent systems with uncertainties, *International Journal of Applied Mathematics and Computer Science* **31**(4): 635–645, DOI: 10.34768/amcs-2021-0044.

Poznyak, A., Polyakov, A. and Azhmyakov, V. (2014). *Attractive Ellipsoids in Robust Control*, Springer, Boston.

Rudenko, O. and Hedberg, C. (2013). Strong and weak nonlinear dynamics: Models, classification, examples, *Acoustical Physics* **59**(6): 644–650.

Ruderman, M. (2015). Presliding hysteresis damping of LuGre and Maxwell-slip friction models, *Mechatronics* **30**: 225–230, DOI: 10.1016/j.mechatronics.2015.07.007.

Sánchez, B., Cuvas, C., Ordaz, P., Santos-Sánchez, O. and Poznyak, A. (2019). Full-order observer for a class of nonlinear systems with unmatched uncertainties: Joint attractive ellipsoid and sliding mode concepts, *IEEE Transactions on Industrial Electronics* **67**(7): 5677–5686.

Shtessel, Y., Edwards, C., Fridman, L. and Levant, A. (2014). *Sliding Mode Control and Observation*, Springer, New York.

Silva, J.M.A.-D., Edwards, C. and Spurgeon, S.K. (2009). Sliding-mode output-feedback control based on LMIs for plants with mismatched uncertainties, *IEEE Transactions on Industrial Electronics* **56**(9): 3675–3683.

Tsinias, J. and Theodosis, D. (2016). Luenberger-type observers for a class of nonlinear triangular control systems, *IEEE Transactions on Automatic Control* **61**(12): 3797–3812.

Utkin, V., Poznyak, A., Orlov, Y.V. and Polyakov, A. (2020). *Road Map for Sliding Mode Control Design*, Springer, Cham.

Zhang, H., Zhao, X., Zhang, L., Niu, B., Zong, G. and Xu, N. (2022). Observer-based adaptive fuzzy hierarchical sliding mode control of uncertain under-actuated switched nonlinear systems with input quantization, *International Journal of Robust and Nonlinear Control* **32**(14): 8163–8185.

Patricio Ordaz received his PhD degree in automatic control from CINVESTAV, Mexico City, in 2012. He is currently a professor at the Autonomous University of Hidalgo State. His research interests are in stability analysis of linear and non-linear systems, optimal control, nonlinear control, robust control, adaptive control, system identification and observation, regulation and stabilization of electromechanical and underactuated systems.

Hugo Romero obtained his BS degree in electrical engineering from Instituto Tecnológico de Pachuca, Mexico, in 1996, his MSc degree in electrical engineering (automatic control) from CINVESTAV, Mexico City, Mexico, in 2001, and his PhD degree in automatic control from the University of Technology of Compigne, France, in 2008. He is currently a professor at the Autonomous University of Hidalgo State, Pachuca, Mexico. His present research interests include computer vision, real-time control applications, nonlinear dynamics and control, unmanned aerial vehicles, embedded systems and underactuated mechanical systems.

Carlos Cuvas is an electrical engineer, who graduated from the Technological Institute of Pachuca, Hidalgo, Mexico, in 2003. He received his MS degree from the National Polytechnic Institute, Mexico City, in 2006, and his PhD degree from CINVESTAV, Mexico City, in 2015. He is currently a professor at the Autonomous University of Hidalgo State, Mexico. His research interests include systems with delays, robust control, linear and nonlinear systems, control systems theory and stability analysis.

Omar Sandre received his PhD in electronics from the National Institute for Astrophysics, Optics, and Electronics (INAOE), Puebla, Mexico, in 2017. He is currently a professor of the CONAHCYT research program *Researchers by Mexico* commissioned at the Autonomous University of Hidalgo State (UAEH). His research interests include model predictive control, embedded control systems, and control of power electronics.

Appendix

A1. Proof of Proposition 2

First, note that following equation is fulfilled:

$$\begin{aligned}\dot{\sigma}(t) = \mathbf{K}_1 \{&\mathbf{A}_{11}\hat{x}_1 + \mathbf{A}_{12}\hat{x}_2 + \mathbf{L}_1\mathbf{C}_1 e_1 \\ &+\mathbf{L}_1\mathbf{C}_2 e_2 + +\mathbf{L}_1\xi_y\} + \mathbf{K}_2\{\mathbf{A}_{21}\hat{x}_1 \\ &+\mathbf{A}_{22}\hat{x}_2 + \mathbf{L}_2\mathbf{C}_1 e_1 \\ &+\mathbf{L}_2\mathbf{C}_2 e_2 + \mathbf{L}_2\xi_y + u\} + \dot{u}.\end{aligned} \tag{A1}$$

By using the control action (13), the time derivative of $V(\sigma(t))$ along the trajectories (A1) is given by

$$\dot{V}_1(\sigma(t)) = \sigma^{\intercal}(t)\mathbf{K}_5\xi_y(x,t) - \sigma^{\intercal}(t)\boldsymbol{\rho}\text{sign}(\sigma(t)), \tag{A2}$$

where $\mathbf{K}_5 = \mathbf{K}_1\mathbf{L}_1 + \mathbf{K}_2\mathbf{L}_2$. In view of (A2), we get

$$\begin{aligned}\dot{V}_1(\sigma(t)) \leq \|\sigma(t)\| \cdot \|\mathbf{K}_5\xi_y(x,t)\| \\ - \sigma^{\intercal}(t)\boldsymbol{\rho}\text{sign}(\sigma(t)).\end{aligned} \tag{A3}$$

Using the assumption $\|\mathbf{K}_5\xi_y(x,t)\| \leq \delta_1 < \infty$,

$$\dot{V}_1(\sigma(t)) \leq \|\sigma(t)\| \cdot \delta_1 - \sigma^{\intercal}(t)\boldsymbol{\rho}\text{sign}(\sigma(t)). \tag{A4}$$

Thus, by using the well-known norm in the Hilbert space of finite-dimensional matrices,[4] the product $\sigma^{\intercal}(t)\boldsymbol{\rho}\text{sign}(\sigma(t))$ yields

$$\begin{aligned}\sigma^{\intercal}(t)\boldsymbol{\rho}\text{sign}(\sigma(t)) &:= \langle\sigma(t), \boldsymbol{\rho}\text{sign}(\sigma(t))\rangle \\ &= \text{trace}\{\boldsymbol{\rho}\}\|\sigma(t)\|.\end{aligned} \tag{A5}$$

Moreover, since the trace operator is the sum of all matrix eigenvalues, if $\boldsymbol{\rho}$ is a positive definite matrix and $\lambda_{\min}(\boldsymbol{\rho}) \leq \text{trace}\{\boldsymbol{\rho}\}$, we have

$$\begin{aligned}\dot{V}_1(\sigma(t)) &\leq \|\sigma(t)\| \cdot \delta_1 - \delta \cdot \|\sigma(t)\| \\ &= -(\delta - \delta_1)\|\sigma(t)\|,\end{aligned} \tag{A6}$$

where $\delta := \lambda_{\min}(\boldsymbol{\rho})$. If $0 < \varkappa = \delta - \delta_1$, we get

$$\dot{V}_1(\sigma(t) \leq -\alpha\|\sigma(t)\| = -\varkappa\sqrt{2}\, V_1^{\frac{1}{2}}(\sigma(t)), \tag{A7}$$

and the solution along the time interval $\tau \in [t_0, t)$ of the previous differential inequality is

$$V_1^{\frac{1}{2}}(\sigma(t)) \leq V_1^{\frac{1}{2}}(\sigma(t_0)) - \frac{\varkappa}{\sqrt{2}}(t - t_0), \tag{A8}$$

which means that the sliding variable converges to the origin in finite time

$$t_r = \frac{\sqrt{2}}{\varkappa}V_1^{\frac{1}{2}}(\sigma(t_0)) + t_0.$$

When $t \geq t_r$, the sliding motion $\sigma = \bar{0}_m$ is reached. This means that after the time t_r, the sliding surface yields $\bar{0}_m = \mathbf{K}\hat{x} + u$, and the control law becomes to the linear form $u = -\mathbf{K}_1\hat{x}_1 - \mathbf{K}_2\hat{x}_2$. Additionally, the system trajectory in the sliding manifold implies that $\dot{\sigma}(t) = \bar{0}_m$, which means

$$\xi_y = \mathbf{K}_5^{\intercal}\left(\mathbf{K}_5\mathbf{K}_5^{\intercal}\right)^{-1}\boldsymbol{\rho}\text{sign}(\sigma(t)). \tag{A9}$$

Finally considering (A2), it is evident that $\mathbf{K}_5\xi_y(x,t) = \mathbf{K}_5\mathbf{K}_5^{\intercal}\left(\mathbf{K}_5\mathbf{K}_5^{\intercal}\right)^{-1}\boldsymbol{\rho}\text{sign}(\sigma(t))$. Then introducing (A9) in (3) results in (15), and the proposition is proven.

[4]The operator $\langle\cdot,\cdot\rangle$ denotes the inner product for two n-dimensional vectors.

A2. Proof of Proposition 3

The time derivative of the storage function $V_2(z)$ along the system trajectories (16) is given by

$$\begin{aligned}\dot{V}_2(z) = z^{\intercal}\left\{\mathbf{P}_1\boldsymbol{\mathcal{A}} + \boldsymbol{\mathcal{A}}^{\intercal}\mathbf{P}_1\right\}z \\ + 2z^{\intercal}\mathbf{P}_1\boldsymbol{\mathcal{F}}\bar{\xi}(x,t).\end{aligned} \tag{A10}$$

By adding and subtracting the terms $\alpha V_2(z)$, $\varepsilon_1\|\xi_y(x,t)\|^2$, $\varepsilon_2\|\xi_x(x,t)\|^2$, for some positive scalars α, ε_1 and ε_2, we have

$$\begin{aligned}\dot{V}_2(z) = \bar{z}^{\intercal}\begin{bmatrix}\mathbf{M}_{11} & \mathbf{P}_2\mathbf{L}\mathbf{C} & \mathbf{P}_2\mathbf{L} & \mathbf{0}_{n\times n} \\ \mathbf{C}^{\intercal}\mathbf{L}^{\intercal}\mathbf{P}_2 & \mathbf{M}_{22} & -\mathbf{P}_3\mathbf{L} & \mathbf{P}_3 \\ \mathbf{L}^{\intercal}\mathbf{P}_2 & -\mathbf{L}^{\intercal}\mathbf{P}_3 & -\varepsilon_1\mathbf{I}_p & \mathbf{0}_{p\times n} \\ \mathbf{0}_{n\times n} & \mathbf{P}_3 & \mathbf{0}_{n\times p} & -\varepsilon_2\mathbf{I}_n\end{bmatrix}\bar{z} \\ - \alpha V_2(z) + \varepsilon_1\|\xi_y(x,t)\|^2 \\ + c_1\varepsilon_2 + c_2\varepsilon_2\|x\|^2,\end{aligned} \tag{A11}$$

where

$$\bar{z}^{\intercal} := \begin{bmatrix}\hat{x}^{\intercal} & e^{\intercal} & \xi_y^{\intercal}(x,t) & \xi_x^{\intercal}(x,t)\end{bmatrix},$$

$$\mathbf{M}_{11} = \mathbf{P}_2(\mathbf{A} - \mathbf{B}\mathbf{K}) + (\mathbf{A}^{\intercal} - \mathbf{K}^{\intercal}\mathbf{B}^{\intercal})\mathbf{P}_2 + \alpha\mathbf{P}_2,$$

$$\mathbf{M}_{22} = c\mathbf{P}_3(\mathbf{A} - \mathbf{L}\mathbf{C}) + (\mathbf{A}^{\intercal} - \mathbf{C}^{\intercal}\mathbf{L}^{\intercal})\mathbf{P}_3 + \alpha\mathbf{P}_3.$$

From the error estimate $e = x - \hat{x}$, it is evident that $x = e + \hat{x} = \begin{bmatrix}\mathbf{I}_n & \mathbf{I}_n & \mathbf{0}_{p\times p} & \mathbf{0}_{n\times n}\end{bmatrix}\bar{z}$. In this way,

$$\begin{aligned}\dot{V}_2(z) = \bar{z}^{\intercal}\mathbf{W}\bar{z} - \alpha V_2(z) \\ + \varepsilon_2\|\xi_y(x,t)\|^2 + c_1\varepsilon_1.\end{aligned} \tag{A12}$$

Note that, if $\mathbf{W}$ is a negative definite matrix, then $\dot{V}_2(z) < -\alpha V_2(z) + \varepsilon_2\|\xi_y(x,t)\|^2 + c_1\varepsilon_1$. On the other hand, $\|\xi_y(x,t)\|^2 = \text{sign}^{\intercal}(\sigma)\boldsymbol{\rho}^{\intercal}\left(\mathbf{K}_5\mathbf{K}_5^{\intercal}\right)^{-\intercal}\boldsymbol{\rho}\text{sign}(\sigma) = \mu$. Thus, if there exists a set of solutions (ε_1, ε_2 α, $\mathbf{P}$, $\mathbf{K}$), such that the matrix inequality $\mathbf{W} < 0$ is fulfilled, then (8) holds. This means that the initial time of the storage function $V_2(z)$ is t_r. Consequently, following inequality is fulfilled:

$$\begin{aligned}&V_2(z(t)) \\ &\leq \frac{\beta}{\alpha} + \left(V_2(z(t_r)) - \frac{\beta}{\alpha}\right)\exp\left\{-\alpha(t - t_r)\right\},\end{aligned} \tag{A13}$$

for all $t_0 \leq t_r$, $t \in \mathbb{R}^+$, where β is defined by (19).

The previous result indicates that, independently of the initial time (in this case t_r), if the matrix inequality (18) holds, the system trajectories $x(t)$ belong to an ellipsoid $\mathcal{E}(0, \bar{\mathbf{P}}^{-1})$, with ellipsoidal matrix $\bar{\mathbf{P}} = \frac{\alpha}{\beta}\mathbf{P}$. In fact, from Proposition 1 and Theorem 1, trajectories reach, involved by an exponential bound, an invariant set

$$\Omega = \left\{z : \|z\| \leq \sqrt{\frac{\beta}{\alpha}\lambda_{\max}\mathbf{P}^{-1}}\right\},$$

with the arriving rate given by α. Moreover, notice that for sufficiently small $\eta > 0$, under assumption (A13),

$$t_{r_2} \leq T = \frac{1}{\alpha} \ln \left\{ 1 - \frac{\alpha}{\beta} \left[V(z_{t_r}) + \eta \right] \right\} + t_r,$$

and the *UUB*-Stability of the system trajectories around the origin is concluded, see Definition 2.

A3. Proof of Proposition 4

Apply the non-singular transformation

$$\mathcal{W} = -\mathbf{M}^\intercal \mathbf{W} \mathbf{M},$$

where $\mathbf{M} = \text{diag}([\mathbf{P}_2^{-1}\mathbf{P}_3,\ \mathbf{I},\ \mathbf{I},\ \mathbf{I}])$, the matrix $\mathcal{W}$ is positive definite, having the following structure:

$$\begin{aligned}
\mathcal{W} &= \begin{bmatrix} \mathcal{W}_{11} & -\mathbf{P}_3\mathbf{L}\mathbf{C} & -\mathbf{P}_3\mathbf{L} & \mathbf{0}_{n\times n} \\ -\mathbf{C}^\intercal\mathbf{L}^\intercal\mathbf{P}_3 & \mathcal{W}_{22} & \mathbf{P}_3\mathbf{L} & -\mathbf{P}_3 \\ -\mathbf{L}^\intercal\mathbf{P}_3 & \mathbf{L}^\intercal\mathbf{P}_3 & \varepsilon_1\mathbf{I}_p & \mathbf{0}_{p\times n} \\ \mathbf{0}_{n\times n} & -\mathbf{P}_3 & \mathbf{0}_{n\times p} & \varepsilon_2\mathbf{I}_n \end{bmatrix}, \\
\mathcal{W}_{11} &= \mathbf{P}_3(\mathbf{B}\mathbf{K} - \mathbf{A})\mathbf{P}_2^{-1}\mathbf{P}_3 \\
&\quad + \mathbf{P}_3\mathbf{P}_2^{-1}\left(\mathbf{K}^\intercal\mathbf{B}^\intercal - \mathbf{A}^\intercal\right)\mathbf{P}_3 \\
&\quad - \alpha\mathbf{P}_3\mathbf{P}_2^{-1}\mathbf{P}_3 - c_2\varepsilon_2\mathbf{P}_3\mathbf{P}_2^{-2}\mathbf{P}_3, \\
\mathcal{W}_{22} &= \mathbf{P}_3\left(\mathbf{L}\mathbf{C} - \mathbf{A}\right) + \left(\mathbf{C}^\intercal\mathbf{L}^\intercal - \mathbf{A}^\intercal\right)\mathbf{P}_3 \\
&\quad - \alpha\mathbf{P}_3 + c_2\varepsilon_2\mathbf{I}_n.
\end{aligned} \tag{A14}$$

By selecting

$$\begin{aligned}
\mathbf{Q}^{-1} < (\mathbf{B}\mathbf{K}-\mathbf{A})\mathbf{P}_2^{-1} + \mathbf{P}_2^{-1}(\mathbf{K}^\intercal\mathbf{B}^\intercal \\
-\mathbf{A}^\intercal) - \alpha\mathbf{P}_2^{-1} - c_2\varepsilon_2\mathbf{P}_2^{-2},
\end{aligned}$$

from Schur's complement, we get (A15). Note that previous inequality is equivalent to

$$\begin{aligned}
\mathbf{H} = \Bigg[& (\mathbf{B}\mathbf{K} - \mathbf{A})\mathbf{P}_2^{-1} + \mathbf{P}_2^{-1}(\mathbf{K}^\intercal\mathbf{B}^\intercal - \mathbf{A}^\intercal) - \alpha\mathbf{P}_2^{-1} \\
& \mathbf{I}_n \\
& \mathbf{I}_n \\
& \mathbf{Q} \Bigg] - \begin{bmatrix} \mathbf{P}_2^{-1} \\ \mathbf{0}_{n\times n} \end{bmatrix} c_2\varepsilon_2\mathbf{I}_n \begin{bmatrix} \mathbf{P}_2^{-1} & \mathbf{0}_{n\times n} \end{bmatrix}.
\end{aligned} \tag{A16}$$

By using Schur's complement, another inequality is obtained,

$$\begin{aligned}
0 < \Bigg[& (\mathbf{B}\mathbf{K} - \mathbf{A})\mathbf{P}_2^{-1} + \mathbf{P}_2^{-1}(\mathbf{K}^\intercal\mathbf{B}^\intercal - \mathbf{A}^\intercal) - \alpha\mathbf{P}_2^{-1} \\
& \mathbf{I}_n \\
& \mathbf{P}_2^{-1} \\
& \begin{matrix} \mathbf{I}_n & \mathbf{P}_2^{-1} \\ \mathbf{Q} & \mathbf{0}_{n\times n} \\ \mathbf{0}_{n\times n} & \frac{1}{c_2\varepsilon_2}\mathbf{I}_n \end{matrix} \Bigg].
\end{aligned} \tag{A17}$$

which means that, from (A14), the inequality (A18) is fulfilled. by defining $\mathbf{R} = \mathbf{P}_3\mathbf{Q}^{-1}\mathbf{P}_3$, for some $0 < \mathbf{R}$. Thus, by adding and subtracting the positive matrix $0 < \mathbf{Q} \in \mathbb{R}^{n\times n}$, here we get $\mathbf{R} + \mathbf{Q} = \mathbf{P}_3\mathbf{Q}^{-1}\mathbf{P}_3 + \mathbf{Q}$, and therefore $\mathbf{P}_3\mathbf{Q}^{-1}\mathbf{P}_3 + \mathbf{Q}$ is a positive definite matrix, too. Recall the $\mathbf{\Lambda}$-inequality $\mathcal{X}^\intercal\mathcal{Y} + \mathcal{Y}^\intercal\mathcal{X} \leq \mathcal{X}^\intercal\mathbf{\Lambda}^{-1}\mathcal{X} + \mathcal{Y}^\intercal\mathbf{\Lambda}\mathcal{Y}$, which is valid for any $\mathcal{X} \in \mathbb{R}^{n\times q}$, $\mathcal{Y} \in \mathbb{R}^{n\times q}$ and $0 < \mathbf{\Lambda} \in \mathbb{R}^{q\times q}$. By selecting $\mathcal{X} = \mathbf{P}_3$, $\mathcal{Y} = \mathbf{I}_n$, and $\mathbf{\Lambda} = \mathbf{Q}$, this implies that $\mathbf{P}_3^\intercal + \mathbf{P}_3 \leq \mathbf{P}_3^\intercal\mathbf{Q}^{-1}\mathbf{P}_3 + \mathbf{Q}$, which means $\mathbf{P}_3^\intercal + \mathbf{P}_3 \leq \mathbf{R} + \mathbf{Q} = \mathbf{P}_3^\intercal\mathbf{Q}^{-1}\mathbf{P}_3 + \mathbf{Q}$, and the LMI (A19) obtained.

$$0 < \mathbf{R} + \mathbf{Q} - 2\mathbf{P}_3.$$

In this sense, if (A17)–(A19) hold, the positivity of matrix $\mathcal{W}$ is guaranteed. Furthermore, based on Theorem 2 and using the change of variable $\mathbf{X} = \mathbf{P}_2^{-1}$, from (A17) it follows that

$$\begin{aligned}
\mathbf{\Psi}_2 = \Bigg[& \mathbf{A}\mathbf{X} + \mathbf{A}^\intercal\mathbf{X} - \mathbf{B}\mathbf{K}\mathbf{X} - \mathbf{X}\mathbf{K}^\intercal\mathbf{B}^\intercal + \alpha\mathbf{X} \\
& \mathbf{0}_{n\times n} \\
& \mathbf{0}_{n\times n} \\
& \begin{matrix} \mathbf{0}_{n\times n} & \mathbf{0}_{n\times n} \\ -\mathbf{Q} & \mathbf{0}_{n\times n} \\ \mathbf{0}_{n\times n} & -\frac{1}{c_2\varepsilon_2}\mathbf{I}_n \end{matrix} \Bigg],
\end{aligned} \tag{A20}$$

and

$$\boldsymbol{\mathcal{P}}_2^\intercal\mathbf{\Theta}_2^\intercal\boldsymbol{\mathcal{Q}}_2 := \begin{bmatrix} \mathbf{0}_{n\times n} & -\mathbf{I} & -\mathbf{X} \\ \mathbf{0}_{n\times n} & \mathbf{0}_{n\times n} & \mathbf{0}_{n\times n} \\ \mathbf{0}_{n\times n} & \mathbf{0}_{n\times n} & \mathbf{0}_{n\times n} \end{bmatrix},$$

where the matrices $\boldsymbol{\mathcal{P}}_2$, $\mathbf{\Theta}_2$ and $\boldsymbol{\mathcal{Q}}_2$ are selected as $\boldsymbol{\mathcal{P}}_2 = \begin{bmatrix} \mathbf{0}_{n\times n} & \mathbf{0}_{n\times n} & \mathbf{I}_n \end{bmatrix}$, $\mathbf{\Theta}_2 = \mathbf{X}$, $\boldsymbol{\mathcal{Q}}_2 = \begin{bmatrix} \mathbf{I} & \mathbf{0}_{n\times n} & \mathbf{0}_{n\times n} \end{bmatrix}$.

The null-space of $\boldsymbol{\mathcal{P}}_2$ and $\boldsymbol{\mathcal{Q}}_2$ can be defined as $\boldsymbol{\mathcal{W}}_{P_2}^\intercal = \begin{bmatrix} \mathbf{I}_n & \mathbf{I}_n & \mathbf{0}_{n\times n} \end{bmatrix}$, $\boldsymbol{\mathcal{W}}_{Q_2}^\intercal = \begin{bmatrix} \mathbf{0}_{n\times n} & \mathbf{I}_n & \mathbf{I}_n \end{bmatrix}$, which means that $\boldsymbol{\mathcal{P}}_i\boldsymbol{\mathcal{W}}_{P_i} = \mathbf{0}$, $\boldsymbol{\mathcal{Q}}_i\boldsymbol{\mathcal{W}}_{Q_i} = \mathbf{0}$, $\forall i = 1, 2$. In the same sense, the matrix inequality (A19) can be rewritten in the format (11), and it becomes (A21) and

$$\boldsymbol{\mathcal{P}}_1^\intercal\mathbf{\Theta}_1^\intercal\boldsymbol{\mathcal{Q}}_1 := \begin{bmatrix} \mathbf{0} & \mathbf{P}_3\mathbf{L}\mathbf{C} & -\mathbf{P}_3\mathbf{L} & \mathbf{0} \\ \mathbf{0} & \mathbf{0} & \mathbf{P}_3\mathbf{L} & \mathbf{P}_3 \\ \mathbf{0} & \mathbf{0} & \mathbf{0} & \mathbf{0} \\ \mathbf{0} & \mathbf{0} & \mathbf{0} & \mathbf{0} \end{bmatrix}, \tag{A22}$$

with

$$\begin{aligned}
\mathbf{\Theta}_1 &= \mathbf{I}, \\
\boldsymbol{\mathcal{P}}_1 &= \begin{bmatrix} \mathbf{P}_3 & \mathbf{0} & \mathbf{0} & \mathbf{0} \\ \mathbf{0} & \mathbf{I} & \mathbf{0} & \mathbf{0} \end{bmatrix}, \\
\boldsymbol{\mathcal{Q}}_1 &= \begin{bmatrix} \mathbf{0} & -\mathbf{L}\mathbf{C} & \mathbf{L} & \mathbf{0} \\ \mathbf{0} & \mathbf{0} & \mathbf{P}_3\mathbf{L} & -\mathbf{P}_3 \end{bmatrix}.
\end{aligned}$$

Its null-space is obtained and it has the following structure:

$$\begin{aligned}
\boldsymbol{\mathcal{W}}_{P_1}^\intercal &= \begin{bmatrix} \mathbf{0} & \mathbf{0} & \mathbf{I} & \mathbf{0} \\ \mathbf{0} & \mathbf{0} & \mathbf{0} & \mathbf{I} \end{bmatrix}, \\
\boldsymbol{\mathcal{W}}_{Q_1}^\intercal &= \begin{bmatrix} \mathbf{0} & \mathbf{I} & \mathbf{C}^\intercal & \mathbf{L}^\intercal\mathbf{C}^\intercal \\ \mathbf{I} & \mathbf{0} & \mathbf{0} & \mathbf{0} \end{bmatrix}.
\end{aligned} \tag{A23}$$

$$0 < \begin{bmatrix} (\mathbf{BK}-\mathbf{A})\mathbf{P}_2^{-1} + \mathbf{P}_2^{-1}(\mathbf{K}^\intercal\mathbf{B}^\intercal - \mathbf{A}^\intercal) - \alpha\mathbf{P}_2^{-1} - c_2\varepsilon_2\mathbf{P}_2^{-2} & \mathbf{I}_n \\ \mathbf{I}_n & \mathbf{Q} \end{bmatrix} = \mathbf{H}. \tag{A15}$$

$$\begin{bmatrix} \mathbf{P}_3\mathbf{Q}^{-1}\mathbf{P}_3 & -\mathbf{P}_3\mathbf{LC} & \mathbf{P}_3\mathbf{L}, & \mathbf{0}_{n\times n} \\ -\mathbf{C}^\intercal\mathbf{L}^\intercal\mathbf{P}_3 & \mathbf{P}_3(\mathbf{LC}-\mathbf{A}) + (\mathbf{C}^\intercal\mathbf{L}^\intercal - \mathbf{A}^\intercal)\mathbf{P}_3 - \alpha\mathbf{P}_3 & -\mathbf{P}_3\mathbf{L} & -\mathbf{P}_3 \\ \mathbf{L}^\intercal\mathbf{P}_3 & -\mathbf{L}^\intercal\mathbf{P}_3 & \varepsilon_2\mathbf{I}_p & \mathbf{0}_{p\times n} \\ \mathbf{0}_{n\times n} & -\mathbf{P}_3 & \mathbf{0}_{n\times p} & \varepsilon_1\mathbf{I}_n \end{bmatrix} < \mathcal{W}. \tag{A18}$$

$$\begin{bmatrix} \mathbf{R} & -\mathbf{P}_3\mathbf{LC} & \mathbf{P}_3\mathbf{L} & \mathbf{0}_{n\times n} \\ -\mathbf{C}^\intercal\mathbf{L}^\intercal\mathbf{P}_3 & \mathbf{P}_3(\mathbf{LC}-\mathbf{A}) + (\mathbf{C}^\intercal\mathbf{L}^\intercal - \mathbf{A}^\intercal)\mathbf{P}_3 - \alpha\mathbf{P}_3 & -\mathbf{P}_3\mathbf{L} & -\mathbf{P}_3 \\ \mathbf{L}^\intercal\mathbf{P}_3 & -\mathbf{L}^\intercal\mathbf{P}_3 & \varepsilon_2\mathbf{I}_p & \mathbf{0}_{p\times n} \\ \mathbf{0}_{n\times n} & -\mathbf{P}_3 & \mathbf{0}_{n\times p} & \varepsilon_1\mathbf{I}_p \end{bmatrix} < \mathcal{W}. \tag{A19}$$

$$\mathbf{\Psi}_1 = \begin{bmatrix} -\mathbf{R} & \mathbf{0} & \mathbf{0} & \mathbf{0} \\ \mathbf{0} & \mathbf{P}_3\mathbf{A} + \mathbf{A}^\intercal\mathbf{P}_3 - \mathbf{P}_3\mathbf{LC} - \mathbf{C}^\intercal\mathbf{L}^\intercal\mathbf{P}_3 + \alpha\mathbf{P}_3 & \mathbf{0} & \mathbf{0} \\ \mathbf{0} & \mathbf{0} & -\varepsilon_2\mathbf{I} & \mathbf{0} \\ \mathbf{0} & \mathbf{0} & \mathbf{0} & -\varepsilon_1\mathbf{I} \end{bmatrix}. \tag{A21}$$

Therefore, it is evident that $\mathcal{W}_{P_i}^\intercal\mathbf{\Psi}_i\mathcal{W}_{P_i} < 0$, $\mathcal{W}_{Q_i}^\intercal\mathbf{\Psi}_i\mathcal{W}_{Q_i} < 0$, $\forall i = 1, 2$ are fulfilled, which implies that the feasibility of BMIs (A17)–(A19) is guaranteed.

Finally, from (A17)–(A19), under a change of the variables $\mathbf{X} = \mathbf{P}_2^{-1}$, $\mathbf{Y}_1 = \mathbf{KP}_2^{-1}$, the matrix inequalities $\mathbf{Y}_2 = \mathbf{P}_3\mathbf{L}$, (22)–(23) are obtained, and the proposition is proven.

Received: 25 January 2023
Revised: 13 August 2023
Re-revised: 2 October 2023
Accepted: 9 October 2023